AIAA SciTech Forum
8-12 January 2024, Orlando, FL
AIAA SCITECH 2024 Forum

10.2514/6.2024-2168

Composition and Climate Impacts of increasing launches to Low Earth Orbit

Kostas Tsigaridis[1]
Center for Climate Systems Research, Columbia University, New York, NY, 10025, USA
NASA Goddard Institute for Space Studies, New York, NY, 11222, USA

Robert Field[2]
Applied Physics and Applied Mathematics, Columbia University, New York, NY, 10025, USA
NASA Goddard Institute for Space Studies, New York, NY, 11222, USA

Susanne E. Bauer[3]
NASA Goddard Institute for Space Studies, New York, NY, 10025, USA
Center for Climate Systems Research, Columbia University, New York, NY, 10025, USA

Christopher Maloney[4]
Cooperative Institute for Research in Environmental Sciences, Boulder, CO, 80305, USA
National Oceanic and Atmospheric Administration, Boulder, CO, 80305, USA

Gavin A. Schmidt[5]
NASA Goddard Institute for Space Studies, New York, NY, 10025, USA

Karen H. Rosenlof[6]
National Oceanic and Atmospheric Administration, Boulder, CO, 80305, USA

We present simulations of an Earth system model in which launch vehicles inject gaseous and particulate combustion products into the stratosphere. We considered two plausible scenarios representative for the year 2050, one with 1000 launches per year and another with 10 times more, all of which assuming heavy lift (80 tons to low Earth orbit; LEO) launches using methane as a proxy for liquefied natural gas (LNG) fuel. An industry-standard plume flowfield model was used to predict emission of gaseous species including carbon monoxide, nitrogen oxides, and water vapor. Black carbon was introduced assuming vacuum emission equal 25% of equivalent kerosene engine. The gas emissions showed marginal or insignificant changes in atmospheric composition, while the black carbon emission was found to be the most influential component. Feedbacks involve tropopause and stratospheric warming, followed by a moistening of the stratosphere via tropospheric water vapor intrusions, together with a reduction in global albedo. The fact that LNG-fueled rockets could be a concern from aerosol emissions in our simulations, despite burning more efficiently than conventional fuels,

[1] Research Scientist, 2880 Broadway, New York, NY 10025, USA. kostas.tsigaridis@columbia.edu.
[2] Associate Research Scientist, 2880 Broadway, New York, NY 10025, USA. robert.field@columbia.edu.
[3] Physical Scientist, 2880 Broadway, New York, NY 10025, USA. susanne.e.bauer@nasa.gov.
[4] Research Associate II, 325 Broadway, R/CSL8, Boulder, CO 80305, USA. christopher.maloney@noaa.gov.
[5] Director, 2880 Broadway, New York, NY 10025, USA. gavin.a.schmidt@nasa.gov.
[6] Senior Scientist, 325 Broadway, R/CSL8, Boulder, CO, 80305, USA. karen.h.rosenlof@noaa.gov.

underscores the need to better understand actual black carbon emissions from rocket engines in order to accurately predict the global impacts of launch vehicles on future climate.

I. Introduction

Rocket launches have clear local impacts on atmospheric composition [1], and the number of launches to Low Earth Orbit (LEO) from space agencies and commercial space activities are projected to greatly increase over the next few decades [2]. Better understanding of the broader impacts on air quality, stratospheric ozone, and even climate, under plausible frequency and technological scenarios, including reusable rockets [3], are essential to fully appreciate their potential effects. Depending on the future path of space exploration and utilization, the global rate of orbital launches [4] is projected to accelerate and include an increasing number of heavy lift launch vehicles which would result in much higher rocket engine emissions. Spaceflight is largely unregulated, a situation that could change in the future as the rate of launch emissions increases [5]. Detailed studies of the impacts of emissions from all phases of space flight, from launch to reentry and in all layers of the Earth's atmosphere, are necessary.

The future path of spaceflight technologies and increase in activities are difficult to accurately predict. Nevertheless, current trends and developments can be used to specify plausible future scenarios of launch vehicle emissions from a range of potential technologies (e.g., propellants and payloads) and specific goals (e. g, satellite launches and Mars exploration). Realistic models of rocket engine combustion, afterburning, and launch trajectories provide vertical profiles of emissions, including black carbon particles, nitrogen oxides, water vapor, and other volatiles and relevant byproducts like carbon monoxide. We build upon past work of members of our group [6] performed with the Community Earth System Model (CESM) coupled with the Whole Atmosphere Community Climate Model (WACCM) that includes atmospheric chemistry calculations and aerosol microphysics, and similar work with the Goddard Earth Observing System (GEOS)-Chem model using emissions estimates made for conventional rocket fuel types [7]. Using the National Aeronautics and Space Administration (NASA) Goddard Institute for Space Studies (GISS) Earth system model ModelE, we perform simulations of both the present-day and future (year 2050) climates using realistic emissions for a typical methane fueled heavy lift launch vehicle and plausible, if speculative, number of launches per year. The goal is to both compare the state-of-the-art climate and air quality atmospheric models with high resolution in the vertical and well-resolved stratospheric climate (GISS ModelE and CESM-WACCM), but also to go a step further and understand the future impacts of space launches on climate, as a result of changes induced by the emissions both via gas-phase reactions and aerosol-radiation interactions.

In the work presented here we focus on climate simulations with GISS ModelE of the year 2050 and the type of fuel that will likely dominate space launches in the future, liquefied natural gas (LNG), which is much cleaner in terms of black carbon emissions compared to present-day kerosene launches [8]. The simulations guide future work on rocket engine emissions and illustrate new atmosphere processes that may be uniquely relevant to rocket engine emissions and their impact on climate.

II. Model Description

We use the NASA GISS ModelE Earth System Model (ESM) [9], which is routinely used for transient (e.g. Ref. [10,11]) present-day and future simulations (e.g. Ref. [12]). It is a highly flexible ESM, with version 2.1 used extensively in Coupled Model Intercomparison Project phase 6 (CMIP6; [13]) studies. The horizontal resolution of the model is 2° x 2.5° in latitude and longitude and it extends from the surface to the stratopause, at a pressure of 0.1 hPa (about 65 km in altitude). Our target simulation period was the years around 2050.

Tropospheric chemistry [14,15] includes the inorganic chemistry of reactive oxygen (O_x), nitrogen (NO_x), and hydrogen (HO_x) families as well as CO, and the organic chemistry of methane and higher hydrocarbons using a modified Carbon Bond Mechanism version 4 (CBM4) scheme [16]. The stratospheric chemistry includes chlorine and bromine chemistry together with polar stratospheric clouds [17]. ModelE can include two aerosol schemes: the aerosol microphysical scheme MATRIX [18] and the One-Moment Aerosol (OMA; [11]). MATRIX has the capability to simulate aerosol size distribution and mixing state. We have simulations using both aerosol modules, but only show results with MATRIX here.

In the simulations presented here, we used a prescribed climatological mean ocean state representative for the year 2050, as calculated by coupled atmosphere-ocean simulations of GISS ModelE [12] for the Shared Socio-economic Pathway (SSP) 2-4.5 [19]. The rest of the model setup, including concentrations of greenhouse gases (GHGs), ozone

precursor and aerosol emissions, as well as any other boundary condition needed to simulate the year 2050, were identical with those defined for SSSP2-4.5 in the ScenarioMIP project [19] of CMIP6.

A. Emissions

GISS ModelE requires specification of rocket emissions as a function of altitude and latitude. The gas and particle emission (kg per km)from a launch vehicle is given as a function of altitude by

$$\frac{dM}{dz} = \frac{M(z)}{V_z(z)} EI(x,z) \quad (1)$$

Where M equals the total propellant mass flow of (kg km^{-1}) N launches, V_z is rocket vertical velocity, and $EI(x,z)$ is the emission index for component x as a function of altitude (g kg^{-1}). The emission components of interest are carbon dioxide (CO_2; not used here), carbon monoxide (CO), water vapor (H_2O), hydroxyl radicals (OH; not used here), nitrogen oxide (NO; in the form of NO_x), and black carbon (BC) aerosols. With the model upper boundary at 0.1 hPa (about 65 km altitude) the exact details of the launch trajectory are not important. A typical ascent trajectory for a two stage launch vehicle placing 80 tons into a 188 km altitude orbit with staging at 63 km is used to calculate V_z. The propellant mass flows m of the modeled stage one and two equals 2,200 and 440 kg km^{-1} and $M(z)$ equals $N \cdot m(z)$. The atmosphere model input $M(z)$ equals $N \cdot m(z)$, the number of launches times the propellant flow rate of a single assumed launch vehicle.

The propellants used to calculate $EI(x,z)$ are methane (CH_4) and liquid oxygen (LOX). The launch vehicles in development commonly referred to as "methane fueled" actually use refined liquid natural gas (LNG) that is predominantly CH_4 but includes additional hydrocarbon contaminants. LNG rocket fuel composition varies from engine to engine and little information exists in the open literature regarding exact compositions [20]. The influence of the minor constituents are unlikely to be important for the main gas phase emissions from rockets but might influence minor species' or aerosol emissions. Future work should consider the difference between CH_4 and actual LNG propellant on emissions.

The emission indices $EI(x,z)$ are calculated using an industry standard model that includes the flow structure of the free exhaust plume and the entrainment of ambient air to support secondary combustion [21]. Gas emissions were calculated assuming a rocket engine burning CH_4 and O_2 at a fuel rich mixture ratio of 1.6 and a thrust of 1.76 MN; these results were scaled up to be consistent with the 80 mT to LEO payload assumption. The plume flowfield model is run at 10 km altitude increments between 0 and 70 km altitude where afterburning is no longer is a factor because of low ambient air density. The EIs calculated for this work are in general agreement with other calculations [22].

The emission index of BC is not included in the plume flowfield calculations and so must be estimated from a phenomenological point of view. BC production in rocket engines and subsequent oxidation and consumption in afterburning are difficult problems and are active areas of research. A general model that predicts $EI(BC,z)$ for an arbitrary engine (i.e., combustion cycle, nozzle film cooling, mixture ratio) is not available. An approximate model of afterburning vigor can be constructed using the plume flowfield prediction of CO emission which is consumed during afterburning. The ratio $R(z) = EI(CO,z)/EI(CO,0\,km)$ equals unity at the surface and falls to zero by the tropopause. The profile of BC emission is $EI(BC,z) = (1 - R(z)) \cdot EI(BC,70km)$. The details of the afterburning profile below the tropopause does not significantly affect the simulation results.

Part of the motivation to use LNG as a rocket fuel is that it contains fewer C atoms per H atom, resulting in much less BC production as it burns than kerosene, which also simplifies routine reuse operations. BC emission at the engine nozzle (e. g., before afterburning) for an LNG engine has never been reported in the open literature. Perfect CH_4/O_2 combustion with a closed cycle engine would produce no BC; however real rocket combustion chambers have unmixed regions of non-equilibrium combustion and the use of LNG for engine film cooling means that, though producing less black carbon than a kerosene engine, it is unlikely to produce no BC at all. While acknowledging large uncertainties, we assume vacuum $EI(BC,70km)$ = 7.5 g/kg, one fourth of the value that is commonly assumed for kerosene engines [2].

The number of launches in this work are assumed to be 1K and 10K per year. This would imply a LEO payload launch rate of 80,000 and 800,000 t per year, respectively, approximately 40 and 400 times the current global launch rate. This launch rate is based on informal and unofficial plans for the several large LNG fueled rockets now in development. The likelihood of achieving this order of magnitude of launch rate in the future is unknown but it is not incompatible with the plans of the global spaceflight enterprise.

B. Simulations

We performed 21 simulations, each of which simulated a perpetual year 2050 for 60 years. The first 10 years were considered a spinup and only the last 50 years were used in the analysis. We varied a) the location of the launch site (Cape Canaveral, FL, USA or Māhia, New Zealand), b) the number of launches per year (1k or 10k), and c) the emitted species (BC only, CO only, NO_x only, water only, or all at once). We also performed a control simulation over the same period, in which no rocket launches were included. These are summarized in Table 1, along with the simulation name used here.

Table 1 Description of simulations performed.

Simulation name	Launch location	# of launches/yr	Emitted species
Control	N/A	N/A	N/A
CC1kBC	Cape Canaveral	1k	BC
CC1kCO	Cape Canaveral	1k	CO
CC1kNOx	Cape Canaveral	1k	NO_x
CC1kWater	Cape Canaveral	1k	Water
CC1kALL	Cape Canaveral	1k	BC, CO, NO_x, Water
CC10kBC	Cape Canaveral	10k	BC
CC10kCO	Cape Canaveral	10k	CO
CC10kNOx	Cape Canaveral	10k	NO_x
CC10kWater	Cape Canaveral	10k	Water
CC10kALL	Cape Canaveral	10k	BC, CO, NO_x, Water
NZ1kBC	Māhia	1k	BC
NZ1kCO	Māhia	1k	CO
NZ1kNOx	Māhia	1k	NO_x
NZ1kWater	Māhia	1k	Water
NZ1kALL	Māhia	1k	BC, CO, NO_x, Water
NZ10kBC	Māhia	10k	BC
NZ10kCO	Māhia	10k	CO
NZ10kNOx	Māhia	10k	NO_x
NZ10kWater	Māhia	10k	Water
NZ10kALL	Māhia	10k	BC, CO, NO_x, Water

III.Results and Discussion

It is useful to compare the rocket emissions used here per species with other relevant sources in the model, for perspective. These include direct sources via emissions as prescribed by ScenarioMIP [19] and chemical secondary sources as calculated by the model's gas-phase chemical mechanism and underlying climate. Direct sources can be separated into anthropogenic emissions near the surface, biomass burning (BB) emissions that are uniformly distributed in the boundary layer, and aircraft emissions that are present throughout the troposphere, but mostly in the upper layers near the tropopause.

For BC, the anthropogenic sources near the surface add up to 4.8 Tg a^{-1}, while biomass burning (BB) adds an additional 1.5 Tg a^{-1}. Probably the most relevant to rocket fuel burning sources, aircraft emissions sum up to 0.016 Tg a^{-1}, but less than any other BC source, including rockets, which equals to 0.084 Tg a^{-1} for 10k launches per year (and one tenth of that, i.e. 0.0084 Tg a^{-1}, for 1k launches per year). The picture is similar for the case of CO, where anthropogenic, BB, and aircraft emissions equal to 445, 285, and 1.0 Tg a^{-1}, respectively, which completely dominate the 0.20 Tg a^{-1} of rocket fuel burning sources for 10k launches per year. CO also has a chemical source, active both in the troposphere and the stratosphere, mostly through the oxidation of methane (CH_4) but also other volatile organics; this source from CH_4 oxidation alone adds to another 1031 Tg a^{-1}, based on our control simulation. Emissions from non-rocket injections dominate the NO_x sources as well: 30, 5.5, and 2.0 Tg a^{-1} from anthropogenic, BB, and aircraft, respectively, are used in the model, compared to 0.14 Tg a^{-1} from rocket fuel burning, while a natural surface source from soils contributes to an additional 2.7 Tg a^{-1}. Similar with CO, NO_x has a significant chemical source in the atmosphere, which comes from the photodissociation of molecular nitrogen and oxygen in the presence of lightning, which then combine to form nitrogen oxides, contributing to another 8.3 Tg a^{-1} throughout the troposphere. Water sources are the most complex to address because of the Earth's hydrological cycle, but for the very dry stratosphere, the only source that is relevant to compare against rocket sources is the chemical source from CH_4 oxidation, 663 Tg

a^{-1} in our control simulation, which can be compared against the 18 Tg a^{-1} from rockets for 10k launches per year scenario.

A. CO

The injection of CO from rocket fuel burning increases the CO concentration in the upper stratosphere very substantially over the launch site (Fig. 2 for Cape Canaveral; nearly identical for Māhia (not shown)), with the 1k launches case increasing the model-top CO concentration by over 50%, which increases to a factor of 6.5 in the 10k launches case. What is interesting to see is that CO decreases in the upper stratosphere in all cases where BC is emitted. This is either a decrease from the control in the case where only BC is emitted (black line in Fig. 2), which reaches 5% and 22% for the 1k and 10k launches, respectively, or a reduced increase in the case where both CO and BC are emitted (orange lines in Fig. 2), which is marginal for the 1k case but changes the factor 6.5 increase down to 5.7. This happens due to enhanced chemical depletion of CO by OH radicals, which increase with the BC injection (Fig. 1), due to a resulting more moist stratosphere in that case, as further detailed in Sect. III.D below. The stratospheric warming, which maximizes at around 1 (5) K for the 1k (10k) launches per year case, results to an acceleration of the reaction rate CO + OH by 0.2 (1) % or less (depending on ambient pressure), which is much smaller than the change of CO loss rate caused by the increased OH concentration (Fig. 1).

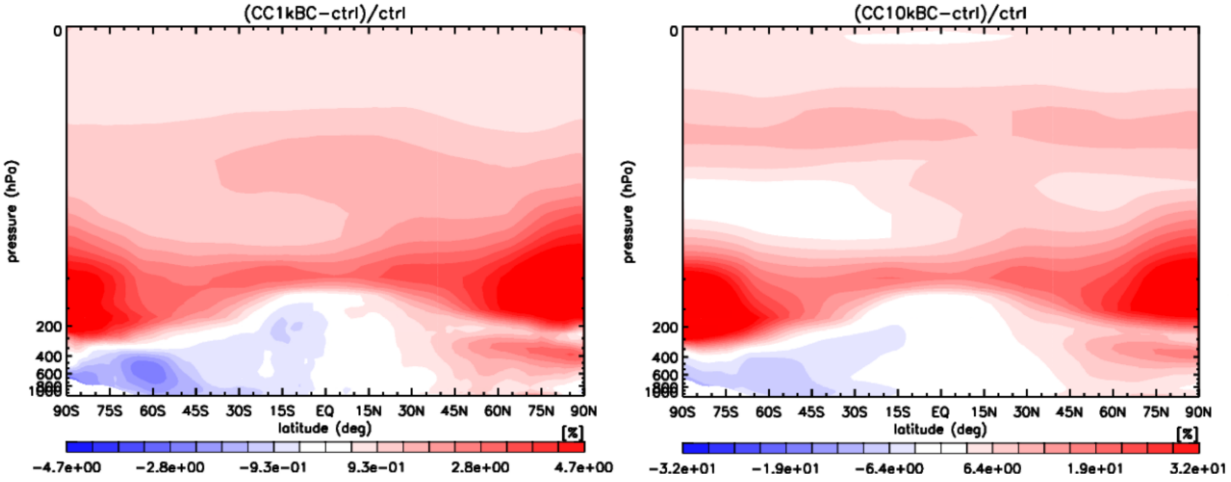

Fig. 1 Zonal mean relative OH radical concentration change [%] due to BC injection in the case of 1k (left) and 10k (right) launches per year as a function of altitude. Note the different scales.

The global mean CO profile changes much less dramatically, since the CO chemical lifetime is not long enough to create a global signal. For the 10k launches scenario CO concentrations near the model top increase by 12%, with the 1k scenario producing only a marginal change from the control simulation where no rocket emissions are used. In the BC-only injection case, CO concentrations near the model top decrease both for the 1k and 10k cases, a direct result of the reduced CO lifetime due to the presence of water that will be detailed below, by as much as 21% for the 10k launches case. The combined BC and CO injection case also leads to decreases of CO concentration near the model top, but with a slightly less decrease at pressures of 1 hPa and higher that reach 13% for the 10k launches case.

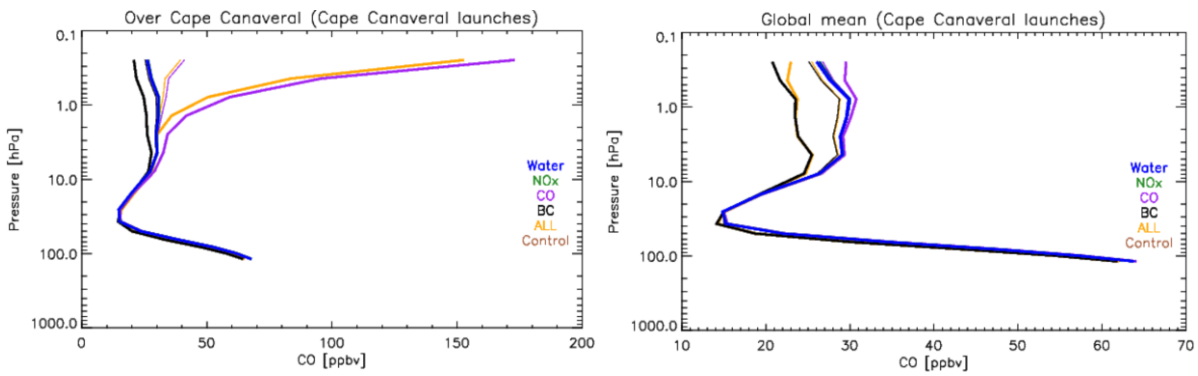

Fig. 2 CO vertical profile in the stratosphere over the Cape Canaveral launch site (left) and global mean (right) when water (blue), NO_x (green), CO (purple), BC (black), and all at once (orange) are emitted from rocket fuel burning. Both 1k launches per year (thin lines) and 10k launches per year (thick lines) are presented. Note the different x-axes range in the two plots.

B. NO_x

In the case of NO_x, there are hardly any changes in the vertical profile in the stratosphere (Fig. 3). The emissions from rocket fuel burning are far too small to affect the photochemistry that dictates the NO_x abundance in the atmosphere, even at the injected locations. As in the case of CO, it is the BC injection that creates some difference, again via the indirect effect of water change, but it is rather small compared to the underlying NO_x concentrations.

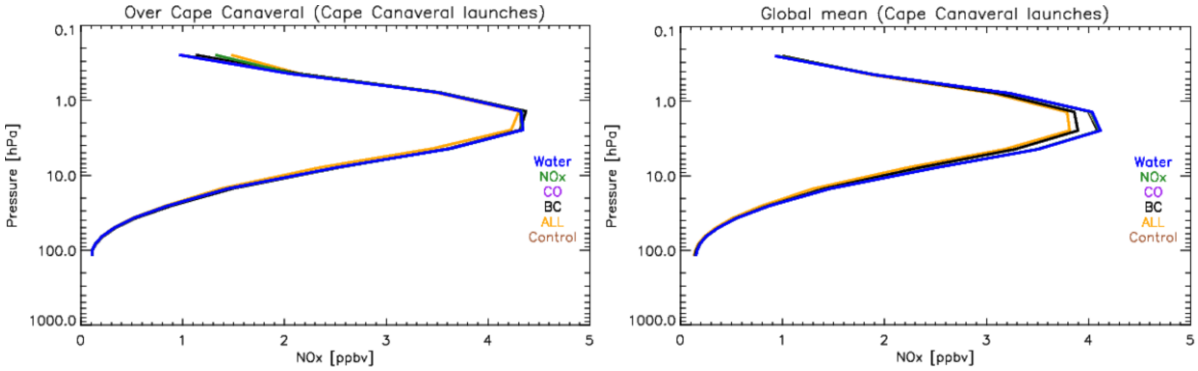

Fig. 3 Same as in Fig. 2 for NOx.

C. Black Carbon

Of all the metrics that were directly affected by the rocket emissions, the most significant is the total BC load in the atmosphere: it went from 92 Gg in the control simulation and those with no BC injection to 110±1 Tg in the simulations where BC is injected following 1k launches per year, to a 3-fold increase of 298±5 Tg in the case of 10k launches. The reason for this increase is that there are practically no removal mechanisms of BC in the stratosphere, other than sedimentation (gravitational settling), which has limited effectiveness for small particles. BC can be effectively removed from the atmosphere only when in the troposphere and below clouds, where wet removal (precipitation) is the dominant BC loss process, by over 90%. In our experiments, rockets are the only source of BC in the stratosphere, contrary to all other emitted species from rocket fuel burning for which significant stratospheric sources are already presents. This, together with the absence of a significant removal mechanism in the stratosphere, increases the BC lifetime in the whole atmosphere from 5.3 days (no rocket emissions) to 6.4 days (1k launches per year) to 17 days (10k launches per year). These changes in burden are clearly visible in the vertical profile of BC as well (Fig. 4), which both locally over the launch location but also globally are increasing stratospheric BC concentrations from practically zero to concentrations that far exceed even the global mean amount found in the troposphere (Fig. 5). The atmospheric composition and climate implications of this increase of stratospheric BC concentration are very extensive, and are discussed in Sect. III.E below.

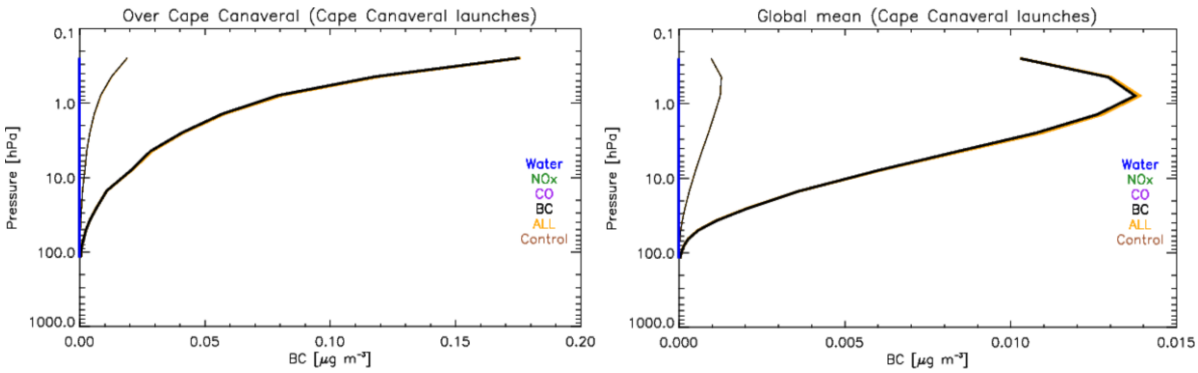

Fig. 4 Same as in Fig. 2 for BC.

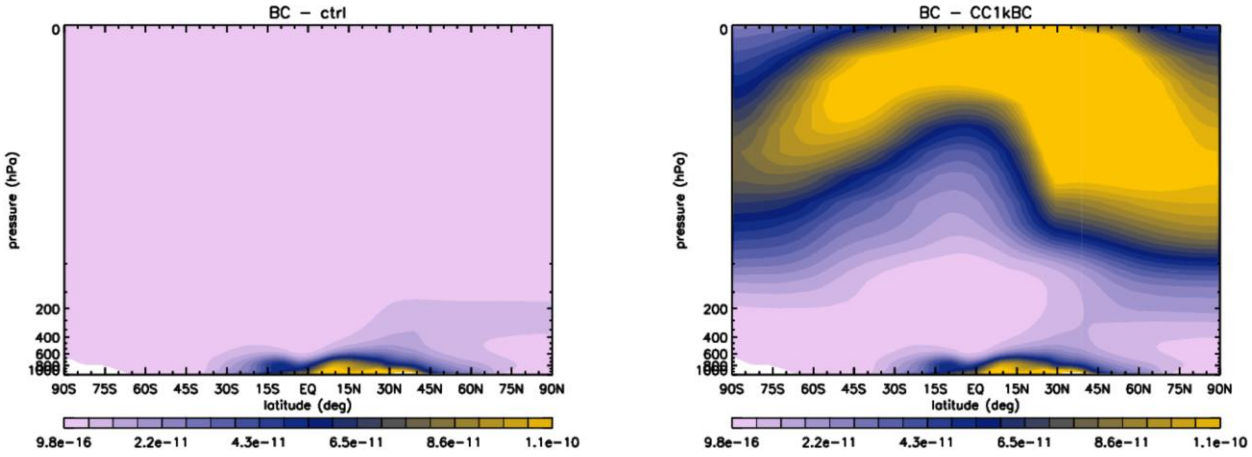

Fig. 5 Zonal mean concentration of BC [mass mixing ratio] in the control experiment (left) and in a simulation with 1k launches per year (right) from Cape Canaveral. For launches from Māhia the hemispheric asymmetry flips, but the general shape is practically identical. The stratosphere appears completely saturated in this color scale for the 10k simulations.

D. Water

The water profile in our simulations is impacted in a more complex way than the other emitted species. Over the launch site the direct injection of water for the 1k launches case increases by up to 4 % without affecting the shape of the profile much, but the 10k launches allow for water accumulation in the upper stratosphere, since there is more being injected than atmospheric circulation can dilute, leading to an increase of 39 % near the model top (blue lines in Fig. 6). These changes get largely diluted when looking at the global mean profile, where only a 5 % increase is calculated at the model top in the 10k launches case. What is interesting though with water is the effect of BC on it, and in particular the 10k simulations, in which stratospheric water concentration increases by up to 12 % over both the launch site and global mean profiles. When both BC and water are injected, the increase is again 12 % over the launch site, and 16 % on the global mean, which shows that the direct injection of water and the BC effect are roughly adding up linearly on the global scale.

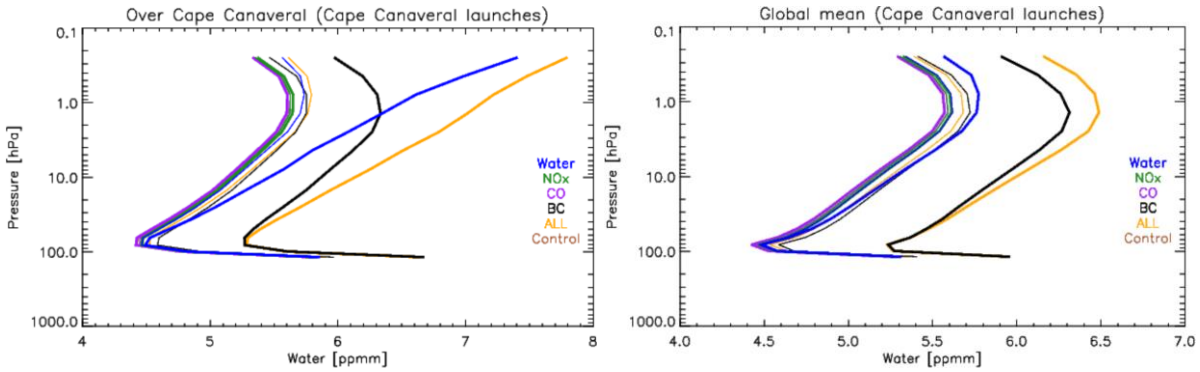

Fig. 6 Same as in Fig. 2 for water vapor.

The importance of BC on the water abundance is striking. The heating of the stratosphere caused by BC absorption in the shortwave, and in particularly around the tropopause, weakens the cold trap that keeps the stratosphere from mixing with the troposphere. This cold trap is the primary reason why the stratosphere is orders of magnitude drier than the troposphere. The increase of the temperature around the tropopause causes water to diffuse more efficiently from the troposphere into the stratosphere, causing the observed stratospheric moistening. The total water vapor amount increases by approximately 7 % when BC is included in the emissions for the 1k launches case, which reaches 50 % for the 10k launches case, compared to the control case, which should be compared with 1 (2) % increase for the 1k (10k) launches case due to a direct water injection. It is important to note that the overall atmospheric burden

of water does not change significantly since stratospheric water is < 0.02 % of the total; although the model calculates a marginal increase of total water load when BC is emitted, this change is not statistically significant.

E. Ozone

One of the key greenhouse gases in the stratosphere is ozone, which responds to both chemical and dynamics changes, and is the main driver of stratospheric temperature. Ozone decreases by 2 and 13 Dobson Units (DU) when only BC is emitted for the 1k and 10k launches per year scenarios, respectively, compared to the 313 DU calculated for the control case.

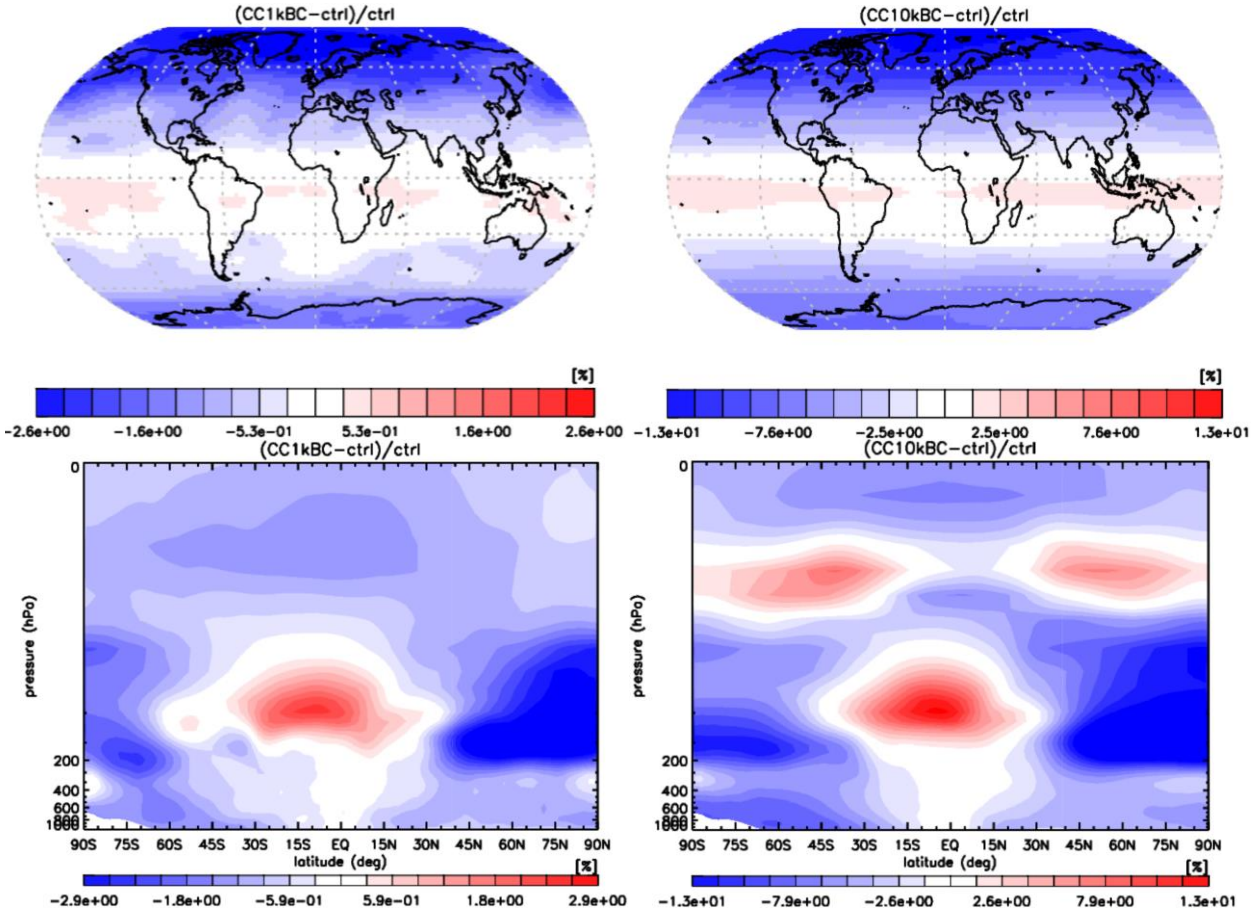

Fig. 7 Column-integrated (top row) and zonal mean (bottom row) ozone changes [%] for the 1k (left column) and 10k (right column) launches per year. Note the difference in scales.

The ozone response is very complex, and is still under investigation. What is interesting to note is that although the bottom half of the stratosphere behaves the same across launches number scenarios, i.e. an ozone loss is calculated at the poles but an ozone production in the tropics, the top half differs substantially across those two cases, where the ozone loss for the 1k launches case becomes a mid-latitude production. More detailed analysis that includes atmospheric circulation changes are needed to understand this response.

F. Climate impacts

The key climate-related effect that is simulated by ModelE is the warming around the tropopause (Fig. 9) that leads to influxes of tropospheric water into the stratosphere. This changes both the radiative balance of the stratosphere (water vapor is a greenhouse gas) but also the chemistry of the whole stratosphere, primarily by enhancing OH radical concentrations (Fig. 1), thus reducing the global burden of key species like CO by 1 % but also GHGs like CH_4 by 0.3 %. Both of those values, albeit small at first inspection, show the global atmospheric reduction by an effect that is concentrated in the mid- to upper stratosphere, and are statistically significant. Note that stratospheric temperature

changes are too modest to directly affect the reaction rates themselves, so chemical kinetic changes are dominated by chemical species abundance changes, rather than temperature-driven reaction rate changes.

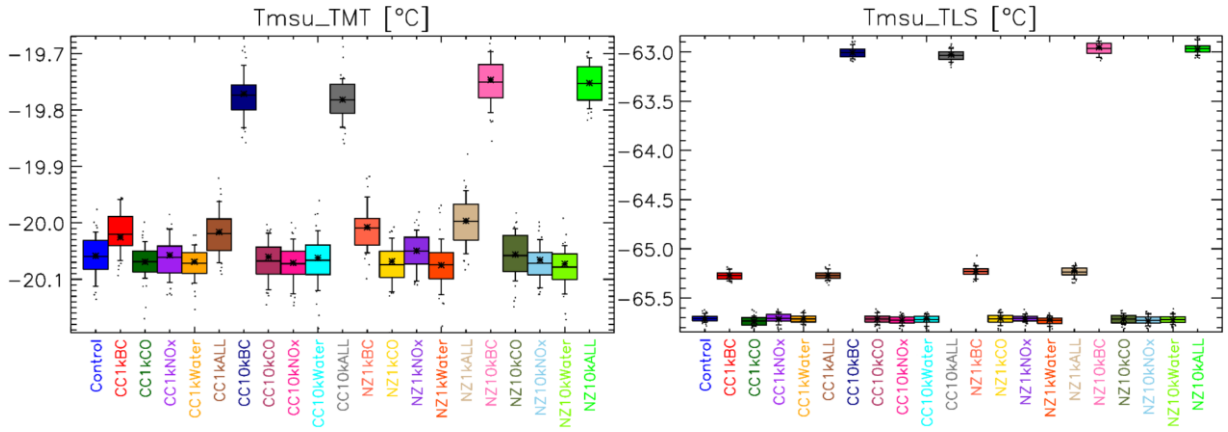

Fig. 8 Box-and-whisker plots of the tropical mid-tropospheric (left) and tropical lower stratospheric temperatures (right) for all model simulations. Stars show the mean, horizontal lines the median, the boxes show the 25/75 percentiles, the error bars show the 9/91 percentiles, and dots present all outlier data.

The global mean change of the tropopause temperature (Fig. 9) is about 0.3 K for the 1k launches simulations and exceeds 1.5 K for the 10k case. Note that these temperature metrics are weighted means from broad regions of the atmosphere designed to mimic results from the Microwave Sounding Unit (MSU) instruments [9,23], and which have global weightings centered on 600 (TMT) and 70 (TLS) hPa (though with substantial tails [24,25]). Although all of these cases lead to increases of water in the upper stratosphere (Fig. 9), the most striking impact is simulated for the 10k launches cases. As already presented in Fig. 6, we can also see here the two 10k simulations in which only water was injected to show a significant increase from the control simulation, which is roughly additive to the effect of 10k launches with BC-only injections, leading to the strongest impact being calculated for the 10k simulations with both BC and water injected. This means that the two effects, direct injection vs. influx from the tropopause, are two disconnected mechanisms in the atmosphere.

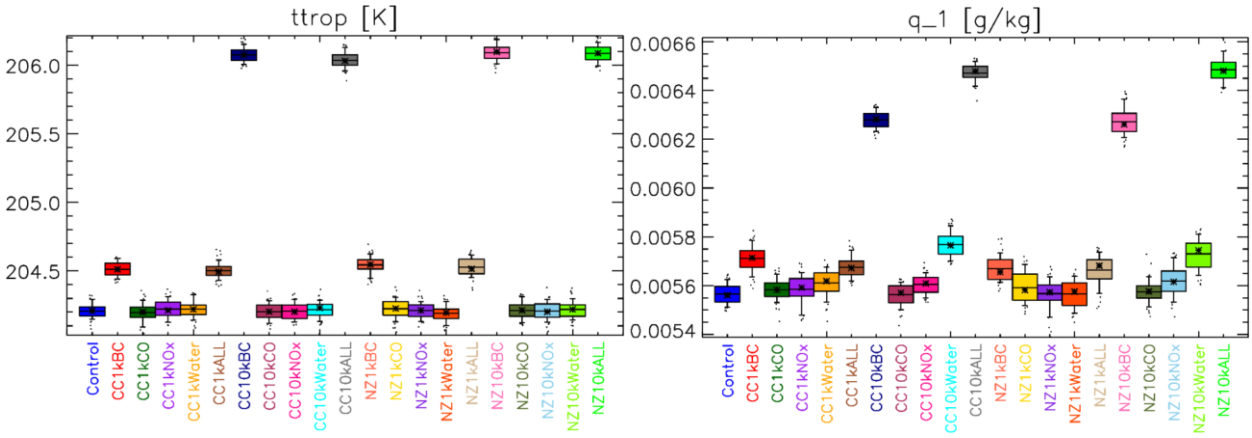

Fig. 9 Same as Fig. 8 for tropopause temperature (left) and water vapor concentration at 1 hPa.

The heating of the upper troposphere presented in Fig. 8 has also tropospheric impacts: high clouds, defined as clouds higher than 440 hPa, form less due to the higher ambient temperatures, resulting in an overall lower planetary albedo (Fig. 10).

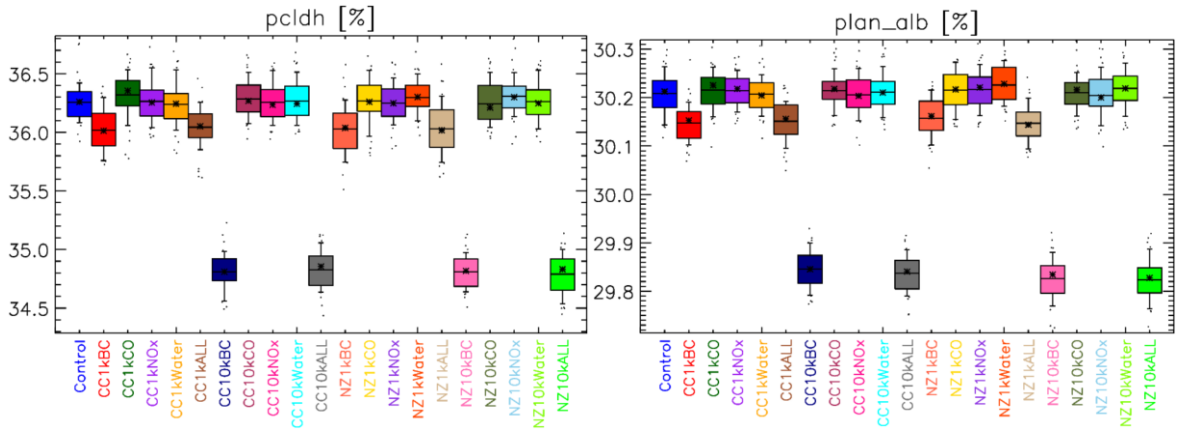

Fig. 10 Same as Fig. 8 for high cloud fraction (left) and planetary albedo (right).

This change is greater in the tropics and less at the poles, with changes at mid-latitudes being statistically insignificant (Fig. 11). These changes though are not enough to change the planetary albedo in the tropics significantly, because of the very bright low clouds there, which do not change statistically significant (not shown). This results in the planetary albedo changes to appear significant only at the poles (Fig. 11).

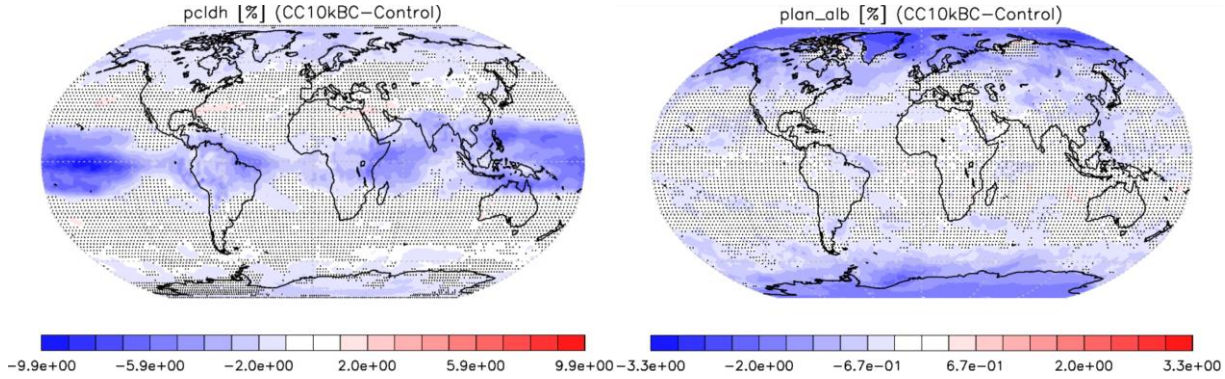

Fig. 11 50-year climatological mean change of high cloud fraction (left) and planetary albedo (right) between the CC10kBC and control simulations. Dots represent areas of statistically insignificant changes.

IV. Conclusion

Looking at annual emission mass alone, it is tempting to conclude that launch vehicle emissions are too small, even insignificant, to have an impact on Earth's atmospheric composition and climate, even for a scenario where 10k launches per year are projected. We presented here why this is not the case, and the role BC plays on this, both directly as a heating agent of the stratosphere, but also as an indirect moisturizing agent of the stratosphere. This process has implications beyond rocket emissions, e.g. for large biomass burning events that reach the troposphere or lower stratosphere (e.g. Ref. [26]) and super-eruptions where sulfate, as a longwave absorber, leads to a similar effect like the shortwave BC absorption does (e.g. Ref. [27]). More chemical effects, e.g. heterogeneous reactions on BC surfaces that can potentially lead to stratospheric ozone changes, will be studied in the future. Further, the changes of stratospheric water vapor, albeit small, have the potential to alter stratospheric circulation [28], something that we will also study in the future.

The simulations further emphasize the need to better understand BC emissions from rocket engines. The predicted response of the atmosphere presented here shows that BC is the determinative emission from rocket engines. The assumed BC mass fraction of 0.7% at the nozzle exit plane (including film cooling) could be larger or smaller in real LNF engines. The applicability of rocket emission simulations to the needs of future researches and policymakers is limited by the accuracy of the understanding of rocket BC emissions and further detailed research using in situ measurements and improved plume models is warranted.

Acknowledgments

All authors acknowledge funding from the Earth Science Division of the NASA Science Mission Directorate. Resources supporting this work were provided by the NASA High-End Computing (HEC) Program through the NASA Center for Climate Simulation (NCCS) at Goddard Space Flight Center. We are also grateful to Martin N. Ross from the Aerospace Corporation for providing us with emission profile data used in all model simulations described here.

References

[1] Dallas, J. A., Raval, S., Alvarez Gaitan, J. P., Saydam, S., and Dempster, A. G., "The Environmental Impact of Emissions from Space Launches: A Comprehensive Review," *Journal of Cleaner Production*, Vol. 255, 2020, p. 120209. https://doi.org/10.1016/j.jclepro.2020.120209

[2] Ross, M. N., and Jones, K. L., "Implications of a Growing Spaceflight Industry: Climate Change," *Journal of Space Safety Engineering*, Vol. 9, No. 3, 2022, pp. 469–477. https://doi.org/10.1016/j.jsse.2022.04.004

[3] Larson, E. J. L., Portmann, R. W., Rosenlof, K. H., Fahey, D. W., Daniel, J. S., and Ross, M. N., "Global Atmospheric Response to Emissions from a Proposed Reusable Space Launch System," *Earth's Future*, Vol. 5, No. 1, 2017, pp. 37–48. https://doi.org/10.1002/2016EF000399

[4] Witze, A., "2022 Was a Record Year for Space Launches," *Nature*, Vol. 613, No. 7944, 2023, pp. 426–426. https://doi.org/10.1038/d41586-023-00048-7

[5] Shutler, J. D., Yan, X., Cnossen, I., Schulz, L., Watson, A. J., Glaßmeier, K.-H., Hawkins, N., and Nasu, H., "Atmospheric Impacts of the Space Industry Require Oversight," *Nature Geoscience*, Vol. 15, No. 8, 2022, pp. 598–600. https://doi.org/10.1038/s41561-022-01001-5

[6] Maloney, C. M., Portmann, R. W., Ross, M. N., and Rosenlof, K. H., "The Climate and Ozone Impacts of Black Carbon Emissions From Global Rocket Launches," *Journal of Geophysical Research: Atmospheres*, Vol. 127, No. 12, 2022, p. e2021JD036373. https://doi.org/10.1029/2021JD036373

[7] Ryan, R. G., Marais, E. A., Balhatchet, C. J., and Eastham, S. D., "Impact of Rocket Launch and Space Debris Air Pollutant Emissions on Stratospheric Ozone and Global Climate," *Earth's Future*, Vol. 10, No. 6, 2022, p. e2021EF002612. https://doi.org/10.1029/2021EF002612

[8] Ross, M., Mills, M., and Toohey, D., "Potential Climate Impact of Black Carbon Emitted by Rockets," *Geophysical Research Letters*, Vol. 37, 2010. https://doi.org/10.1029/2010gl044548

[9] Kelley, M., Schmidt, G. A., Nazarenko, L. S., Bauer, S. E., Ruedy, R., Russell, G. L., Ackerman, A. S., Aleinov, I., Bauer, M., Bleck, R., Canuto, V., Cesana, G., Cheng, Y., Clune, T. L., Cook, B. I., Cruz, C. A., Del Genio, A. D., Elsaesser, G. S., Faluvegi, G., Kiang, N. Y., Kim, D., Lacis, A. A., Leboissetier, A., LeGrande, A. N., Lo, K. K., Marshall, J., Matthews, E. E., McDermid, S., Mezuman, K., Miller, R. L., Murray, L. T., Oinas, V., Orbe, C., García-Pando, C. P., Perlwitz, J. P., Puma, M. J., Rind, D., Romanou, A., Shindell, D. T., Sun, S., Tausnev, N., Tsigaridis, K., Tselioudis, G., Weng, E., Wu, J., and Yao, M.-S., "GISS-E2.1: Configurations and Climatology," *Journal of Advances in Modeling Earth Systems*, Vol. 12, No. 8, 2020, p. e2019MS002025. https://doi.org/10.1029/2019MS002025

[10] Miller, R. L., Schmidt, G. A., Nazarenko, L. S., Bauer, S. E., Kelley, M., Ruedy, R., Russell, G. L., Ackerman, A. S., Aleinov, I., Bauer, M., Bleck, R., Canuto, V., Cesana, G., Cheng, Y., Clune, T. L., Cook, B. I., Cruz, C. A., Del Genio, A. D., Elsaesser, G. S., Faluvegi, G., Kiang, N. Y., Kim, D., Lacis, A. A., Leboissetier, A., LeGrande, A. N., Lo, K. K., Marshall, J., Matthews, E. E., McDermid, S., Mezuman, K., Murray, L. T., Oinas, V., Orbe, C., Pérez García-Pando, C., Perlwitz, J. P., Puma, M. J., Rind, D., Romanou, A., Shindell, D. T., Sun, S., Tausnev, N., Tsigaridis, K., Tselioudis, G., Weng, E., Wu, J., and Yao, M.-S., "CMIP6 Historical Simulations (1850–2014) With GISS-E2.1," *Journal of Advances in Modeling Earth Systems*, Vol. 13, No. 1, 2021, p. e2019MS002034. https://doi.org/10.1029/2019MS002034

[11] Bauer, S. E., Tsigaridis, K., Faluvegi, G., Kelley, M., Lo, K. K., Miller, R. L., Nazarenko, L., Schmidt, G. A., and Wu, J., "Historical (1850-2014) Aerosol Evolution and Role on Climate Forcing Using the GISS ModelE2.1 Contribution to CMIP6," *Journal of Advances in Modeling Earth Systems*, 2020, p. e2019MS001978. https://doi.org/10.1029/2019MS001978

[12] Nazarenko, L. S., Tausnev, N., Russell, G. L., Rind, D., Miller, R. L., Schmidt, G. A., Bauer, S. E., Kelley, M., Ruedy, R., Ackerman, A. S., Aleinov, I., Bauer, M., Bleck, R., Canuto, V., Cesana, G., Cheng, Y., Clune, T. L., Cook, B. I., Cruz, C. A., Del Genio, A. D., Elsaesser, G. S., Faluvegi, G., Kiang, N. Y., Kim, D., Lacis, A. A., Leboissetier, A., LeGrande, A. N., Lo, K. K., Marshall, J., Matthews, E. E., McDermid, S., Mezuman, K., Murray, L. T., Oinas, V., Orbe, C., García-Pando, C. P., Perlwitz, J. P., Puma, M. J., Romanou, A., Shindell, D. T., Sun, S., Tsigaridis, K., Tselioudis, G., Weng, E., Wu, J., and Yao, M.-S., "Future Climate Change Under

SSP Emission Scenarios With GISS-E2.1," *Journal of Advances in Modeling Earth Systems*, Vol. 14, No. 7, 2022, p. e2021MS002871. https://doi.org/10.1029/2021MS002871

[13] Eyring, V., Bony, S., Meehl, G. A., Senior, C. A., Stevens, B., Stouffer, R. J., and Taylor, K. E., "Overview of the Coupled Model Intercomparison Project Phase 6 (CMIP6) Experimental Design and Organization," *Geoscientific Model Development*, Vol. 9, No. 5, 2016, pp. 1937–1958. https://doi.org/10.5194/gmd-9-1937-2016

[14] Shindell, D. T., Grenfell, J. L., Rind, D., Grewe, V., and Price, C., "Chemistry-Climate Interactions in the Goddard Institute for Space Studies General Circulation Model 1. Tropospheric Chemistry Model Description and Evaluation," *Journal of Geophysical Research-Atmospheres*, Vol. 106, No. D8, 2001, pp. 8047–8075. https://doi.org/10.1029/2000jd900704

[15] Shindell, D. T., Faluvegi, G., and Bell, N., "Preindustrial-to-Present-Day Radiative Forcing by Tropospheric Ozone from Improved Simulations with the GISS Chemistry-Climate GCM," *Atmos. Chem. Phys.*, Vol. 3, No. 5, 2003, pp. 1675–1702. https://doi.org/10.5194/acp-3-1675-2003

[16] Gery, M. W., Whitten, G. Z., Killus, J. P., and Dodge, M. C., "A Photochemical Kinetics Mechanism for Urban and Regional Scale Computer Modeling," *Journal of Geophysical Research*, Vol. 94, No. D10, 1989, p. 12925. https://doi.org/10.1029/JD094iD10p12925

[17] Shindell, D. T., Faluvegi, G., Unger, N., Aguilar, E., Schmidt, G. A., Koch, D. M., Bauer, S. E., and Miller, R. L., "Simulations of Preindustrial, Present-Day, and 2100 Conditions in the NASA GISS Composition and Climate Model G-PUCCINI," *Atmospheric Chemistry and Physics*, Vol. 6, 2006, pp. 4427–4459.

[18] Bauer, S. E., Wright, D. L., Koch, D., Lewis, E. R., McGraw, R., Chang, L. S., Schwartz, S. E., and Ruedy, R., "MATRIX (Multiconfiguration Aerosol TRacker of mIXing State): An Aerosol Microphysical Module for Global Atmospheric Models," *Atmos. Chem. Phys.*, Vol. 8, No. 20, 2008, pp. 6003–6035. https://doi.org/10.5194/acp-8-6003-2008

[19] O'Neill, B. C., Tebaldi, C., van Vuuren, D. P., Eyring, V., Friedlingstein, P., Hurtt, G., Knutti, R., Kriegler, E., Lamarque, J.-F., Lowe, J., Meehl, G. A., Moss, R., Riahi, K., and Sanderson, B. M., "The Scenario Model Intercomparison Project (ScenarioMIP) for CMIP6," *Geoscientific Model Development*, Vol. 9, No. 9, 2016, pp. 3461–3482. https://doi.org/10.5194/gmd-9-3461-2016

[20] Al Ghafri, S. Z. S., Swanger, A., Park, K. H., Jusko, V., Ryu, Y., Kim, S., Kim, S. G., Zhang, D., Seo, Y., Johns, M. L., and May, E. F., "Advanced Boil-off Gas Studies of Liquefied Natural Gas Used for the Space and Energy Industries," *Acta Astronautica*, Vol. 190, 2022, pp. 444–454. https://doi.org/10.1016/j.actaastro.2021.10.028

[21] Taylor, M., and Pergament, H., "Standardized Plume Flowfield Model SPF-III," User's Manual, PST TR-51, Propulsion Science and Technology, Inc, East Windsor, NJ, June 2000.

[22] B. Liu, C. Xing, G. Le, P. Dong, and K. Liu, "Investigation of Afterburning Effects on the Thermal Environment of Methane Rocket at Different Altitudes," presented at the 2022 13th International Conference on Mechanical and Aerospace Engineering (ICMAE), 2022. https://doi.org/10.1109/ICMAE56000.2022.9852843

[23] Casas, M. C., Schmidt, G. A., Miller, Ron. L., Orbe, C., Tsigaridis, K., Nazarenko, L. S., Bauer, S. E., and Shindell, D. T., "Understanding Model-Observation Discrepancies in Satellite Retrievals of Atmospheric Temperature Using GISS ModelE," *Journal of Geophysical Research: Atmospheres*, Vol. 128, No. 1, 2023, p. e2022JD037523. https://doi.org/10.1029/2022JD037523

[24] Mears, C. A., and Wentz, F. J., "Sensitivity of Satellite-Derived Tropospheric Temperature Trends to the Diurnal Cycle Adjustment," *Journal of Climate*, Vol. 29, No. 10, 2016, pp. 3629–3646. https://doi.org/10.1175/JCLI-D-15-0744.1

[25] Zou, C.-Z., and Qian, H., "Stratospheric Temperature Climate Data Record from Merged SSU and AMSU-A Observations," *Journal of Atmospheric and Oceanic Technology*, Vol. 33, No. 9, 2016, pp. 1967–1984. https://doi.org/10.1175/JTECH-D-16-0018.1

[26] Schwartz, M. J., Santee, M. L., Pumphrey, H. C., Manney, G. L., Lambert, A., Livesey, N. J., Millán, L., Neu, J. L., Read, W. G., and Werner, F., "Australian New Year's PyroCb Impact on Stratospheric Composition," *Geophysical Research Letters*, Vol. 47, No. 24, 2020, p. e2020GL090831. https://doi.org/10.1029/2020GL090831

[27] Guzewich, S. D., Oman, L. D., Richardson, J. A., Whelley, P. L., Bastelberger, S. T., Young, K. E., Bleacher, J. E., Fauchez, T. J., and Kopparapu, R. K., "Volcanic Climate Warming Through Radiative and Dynamical Feedbacks of SO2 Emissions," *Geophysical Research Letters*, Vol. 49, No. 4, 2022, p. e2021GL096612. https://doi.org/10.1029/2021GL096612

[28] Charlesworth, E., Plöger, F., Birner, T., Baikhadzhaev, R., Abalos, M., Abraham, N. L., Akiyoshi, H., Bekki, S., Dennison, F., Jöckel, P., Keeble, J., Kinnison, D., Morgenstern, O., Plummer, D., Rozanov, E., Strode, S.,

Zeng, G., Egorova, T., and Riese, M., “Stratospheric Water Vapor Affecting Atmospheric Circulation,” *Nature Communications*, Vol. 14, No. 1, 2023, p. 3925. https://doi.org/10.1038/s41467-023-39559-2